Analyst

Accepted Manuscript

Analyst

PAPER

Upconversion Nanoparticles for Ratiometric Fluorescence Detection of Nitrite

Junfen Han,[ab] **Cheng Zhang,**[ab] **Fei Liu,**[c] **Bianhua Liu,**[*b] **Mingyong Han,**[b] **Wensheng Zou,**[b] **Liang Yang**[ab] **and Zhongping Zhang**[*ab]

We have developed a selective upconversion switching method for the ratiometric fluorescence detection of nitrite using upconversion nanoparticles (UCNPs) and an efficient reaction. The green emission (λ_{em} = 539 nm) of $NaYF_4$:Yb^{3+},Er^{3+} nanoparticles can be selectively quenched by the neutral red (NR) dye due 10 to the spectral overlapping between the emission at 539 nm and the absorption of NR, while its red emission (λ_{em} = 654 nm) keeps unchanged. Nitrite can specifically and strongly react with NR to form diazonium salt and lose diazonium group, which can sharply decrease the absorption of NR. Thus, the green emission of $NaYF_4$:Yb^{3+},Er^{3+} can be recovered obviously with the increase of nitrite amount, leading to the visual color changes from red to orange yellow and final green under excitation with 980-15 nm laser. The increase of ratio of emission intensities (I_{539}/I_{654}) is quantitatively correlated to the concentration of nitrite ions. Moreover, the developed method has been successfully applied to real sample detection such as nitrite in drinking water, natural water and meat foods. In particular, the upconversion sensors can efficiently avoid the optical interference of background and thus may provide the more potential applications for the detection of nitrite salts in complex samples.

1. Introduction

People have kept highly alert on the possible contamination of nitrite in food and drinking water, because it is easily produced by the natural or biological conversions of nitrate and nitrogen-containing organics including livestock manure, chemical 25 fertilizers, natural deposits and etc.[1-3] A number of medical issues such as esophageal cancers and blue baby syndrome are associated with unintentional chronic intake of nitrite.[4,5] The U.S. Environmental Protection Agency (EPA) defined the maximum contamination levels of nitrite in drinking water and meat 30 products to be 1 and 200 ppm, respectively,[6] and the analogous guideline value in water set by the World Health Organization (WHO) is 3 ppm.[7] Therefore, the determination of nitrite levels is extremely important in monitoring drinking water and food qualities. The commercial method for nitrite analysis is based on 35 Griess reaction to achieve the spectrophotometric measurement,[8] which involves the diazotization of sulfanilamide by nitrite under acidic conditions, and the coupling of the *in situ* generated diazonium ion with N-(1-naphthyl)ethylenediamine affords azochromophore. Unfortunately, this currently adopted method is 40 time-consuming and usually needs the tedious separation, concentration or beforehand treatment to real samples. It remains a challenge to achieve the simple, rapid detection of nitrite in the interferences of coexisting nitrate and other anions in complicated matrices.

45 Recently, a serial of instruments-based approaches have been developed for the determination of nitrite by chemiluminescence,[9] chromatography,[10] capillary electrophoresis[11] and electrochemistry.[12] In particular, negative chemical ionization GC/MS can determinate nitrite and nitrate in 50 seawater using isotope dilution and derivatization.[13] On the other hand, the recent developments of organic probes and nanosensors have opened a novel avenue to the visual assay of nitrite.[14,15] Reactive aza-dye colorimetric probes can achieve the sensitive detection, quantification and on-site analysis of nitrite ions.[16] 55 Ligand-modified gold nanoparticles and nanorods have been successfully used for the colorimetric detection of nitrite and nitrate in water by the change of color due to their aggregations.[17,18] Similarly, fluorescent gold nanoclusters have also been applied for detection of nitrite.[19,20] In addition, reaction-60 based fluorometric probes, named as chemodosimeters, which involve the target analyte induced fast chemical reactions, have been developed for detection of nitrite.[21] For instance, a rhodamine based fluorogenic chemodosimeter was employed in the trace determination of nitrite.[22] These reported results imply 65 that a simple, sensitive, but suitable for complex samples, approach is highly conceivable and needs further explorations.

Upconversion nanoparticles (UCNPs) doped with certain rare-earth ions have recently attracted considerable attention, in which the low energy near-infrared light (typical, 980 nm) can be 70 converted into a higher energy visible emission through multiple-photon absorption or energy transfer.[23-25] This unique luminescence mechanism allows the UCNPs to exhibit several significant advantages, including narrow spectral emission, excellent emission stability, low damage to analytes, and nearly 75 no autofluorescence interference and photobleaching. To date,

UCNPs has been widely applied in chemosensing[26,27] or imaging applications.[28,29] In particular, several upconversion luminescent resonance energy transfer (LRET) systems have been proposed for the detections of methylmercury,[30] Cu^{2+},[31] and glutathione.[32] Here, we report a selective upconversion switching method for the ratiometric fluorescence detection of nitrite using UCNPs and an efficient reaction. The green emission of $NaYF_4$:Yb^{3+}, Er^{3+} nanoparticles can be selectively quenched by the neutral red (NR) dye due to the spectral overlapping, while its red emission keeps unchanged. Nitrite can specifically and strongly react with NR to form diazonium salt and lose diazonium group, shutting off the energy transfer pathway, and thus the green emission of $NaYF_4$:Yb^{3+}, Er^{3+} can be recovered obviously, leading to the visual color changes from red to orange yellow and final green under excitation with 980-nm laser. This ratiometric fluorescence detection of nitrite shows a high selectivity and sensitivity and is successfully applied to real sample detection.

2. Experimental

2.1 Chemicals

Oleic acid (OA, technical grade, 90%), 1-Octadecene (ODE, technical grade, 90%) and poly(acrylic acid) (PAA, $M_w \approx 1800$) were purchased from Sigma-Aldrich. Diethylene glycol (DEG), methanol, ethanol, toluene, hydrochloric acid (HCl, 37%), NaOH, NH_4F and all the metal salts were supplied by Sinopharm Chemical Reagent Co., Ltd. (Shanghai, China). All of these reagents were used without further purification. $RECl_3$ (RE = Y^{3+}, Yb^{3+}, Er^{3+}) were prepared by dissolving the corresponding rare earth oxides in hydrochloric acid at elevated temperature, followed by evaporating the solvent. Ultrapure water (18.2 MΩ) was produced using Millipore purification system. The lake water was collected from a local reservoir (Hefei, Anhui, China), and the cured meat was directly purchased from a local supermarket.

2.2 Synthesis of hydrophobic OA-capped UCNPs

Hexagonal Phase $NaYF_4$:Yb^{3+}(20%),Er^{3+}(2%) nanoparticles (upconversion nanoparticles, UCNPs) were prepared according to the reported procedures in the literature[33] with slight modifications. In brief, 0.78 mmol of YCl_3·$6H_2O$, 0.20 mmol of $YbCl_3$·$6H_2O$ and 0.02 mmol of $ErCl_3$·$6H_2O$ were mixed with 6 mL oleic acid and 17 mL 1-octadecene in a 50 mL flask under stirring, and the mixture was heated to 160 ºC under vacuum to form a homogeneous solution, and then cooled down to room temperature. 10 mL methanol solution containing NaOH (0.1 g) and NH_4F (0.1482 g) was then dropwisely added into the flask. After stirring for 30 min, the mixing solution was slowly heated to evaporate methanol, degassed at 100 ºC for 10 min, and then heated to 310 ºC under nitrogen atmosphere and kept for 1.5 h. After cooling down naturally, the hydrophobic UCNPs with oleic acid (OA) ligands on the surface were obtained by the precipitation with ethanol and washed with ethanol for three times.

2.3 Conversion of hydrophobic OA-capped UCNPs to hydrophilic PAA-capped UCNPs

The above hydrophobic UCNPs were converted into aqueous phase by a surface ligand-exchange strategy.[34] Typically, 0.5 g of poly(acrylic acid) (PAA) was added into 10 mL of diethylene glycol, and then the mixture was heated to 110 ºC with vigorous stirring under nitrogen to form a clear solution. 2 mL of toluene with 30 mg of the OA-capped UCNPs was injected into the above system. After kept at this temperature for 0.5 h under nitrogen protection, the mixture was heated to 240 ºC for 1 h and subsequently cooled down to room temperature. The white precipitates were obtained via centrifugation, washed three times with ultrapure water, and then dried in a vacuum oven. The prepared PAA-capped UCNPs powder can be well dispersed in water.

2.4 Upconversion luminescence detection of nitrite in water.

Briefly, different amounts of nitrite stock solution were firstly mixed well with 210 μL of neutral red (1.0 mM) and 60 μL of HCl (1.0 M). After reaction under rotation for 10 min, the mixture was buffered with MES solution to pH 6.0. Then, 25 μL of PAA-capped UCNPs aqueous solution (10 mg/mL) was injected into the above mixture. Finally, the volume was quantitatively diluted to 3.0 mL with MES buffer and mixed thoroughly to form a homogeneous solution. The upconversion luminescence (UCL) spectra were recorded on a Fluorolog-3 fluorescence spectrophotometer with a 980-nm diode laser. The spectral intensities were an average of three independent measurements. For comparison, the spectral responses of PAA-capped UCNPs to other ions were also performed by the same procedure as that for NO_2^-.

2.5 Detection of nitrite in real samples

The proposed method was applied to the determination of nitrite including tap water, lake water and cured meat. Tap water and lake water were filtered through 0.45 μm Supor filters. Meat sample was firstly crushed and immersed into 20 mL ultrapure water for one day. Then, the turbid solution was centrifuged at 3000 r/min for 10 min. Finally, the obtained supernatant liquid was filtered with 0.45 μm Supor filters. The above three sample filtrate were firstly spiked by a certain amount of sodium nitrite, and were then mixed well with neutral red in presence of HCl (1.0 M) under rotation for the reaction. Following the above procedures for the detection of nitrite in water, the amounts of nitrite in these samples were determined by the upconversion luminescence of PAA-capped UCNPs.

2.6 Instruments

The crystal structure was analyzed by X-ray powder diffraction (XRD) on a Philips X'Pert Pro with Cu Kα radiation (1.5418 Å). The UCNPs were characterized by transmission electron microscopy (TEM, JEOL 2010) with operating voltage of 200 kV. Fourier transform infrared (FT-IR) and UV–vis absorption spectra were recorded on a Thermo Fisher Nicolet iS10 FT-IR spectrometer and a Shimadzu UV-2550 spectrometer, respectively. Photographs were taken with a Canon 600D digital camera. The UCL spectra were taken using a Fluorolog-3 fluorescence spectrophotometer (Horiba Jobin Yvon, France) equipped with a R928 photomultiplier tube (PMT), in conjunction with an external 980 nm diode laser (Beijing Viasho Technology co. ltd) as the excitation source.

3. Results and discussion

3.1 UCNPs probes

In order to achieve the ratiometric spectral or visual assays to nitrite, we designed a UCNPs probe with dual upconversion emissions (green at 539 nm; red at 654 nm). The better ratiometric effect requires that both emissions are very strong but the red emission as the internal standard is relatively weaker than the changed green emission. Thus, 20% Yb^{3+} and 2% Er^{3+} were doped into the crystalline $NaYF_4$ to meet these spectral requirements. Simultaneously, poly(acrylic acid) (PAA) ligands were modified onto the surface of $NaYF_4$:Yb^{3+}(20%),Er^{3+}(2%) to obtain the aqueous solubility and the interacting ability with neutral red (NR).
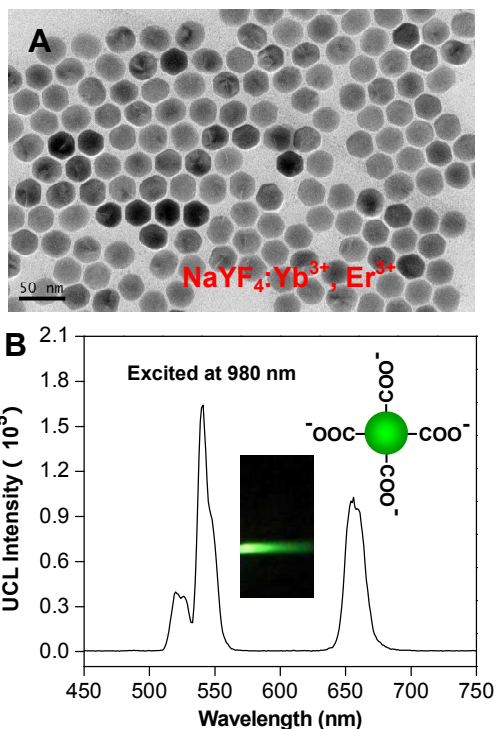
Fig. 1 (A) TEM image of $NaYF_4$:Yb(20%),Er(2%) nanoparticles and (B) the upconversion spectrum of PAA-capped $NaYF_4$:Yb(20%),Er(2%) nanoparticles under excitation at 980 nm. The inset is the optical image with the excitation of 980-nm laser.

Hexagonal $NaYF_4$:Yb^{3+},Er^{3+} nanoparticles are prepared by cothermolysis of rare-earth chlorides in the mixing oleic acid (OA) and 1-octadecene (ODE) at 310 ºC under nitrogen atmosphere according to the reported method.[33] As shown in the transmission electron microscopy (TEM) image, the as-prepared UCNPs nanoparticles are highly uniform, monodisperse, and narrow in size distribution with an average diameter of ~30 nm. The high-resolution TEM (Figure S1-A) reveals the perfect single crystalline structure with the uniform lattice space of (100) planes, and the powder X-ray diffraction (Figure S1-B) is in good agreement with JCPDS (no. 16-0034) of hexagonal $NaYF_4$. The freshly prepared UCNPs are highly hydrophobic due to the surface coverage of OA. The OA-capped UCNPs in toluene were converted into aqueous phase by a surface ligand-exchange with PAA at an elevated temperature under vigorous stirring.[34] The PAA-capped UCNPs can be well-dispersed in water and remain monodispersed (Figure S2). Moreover, Fourier transform infrared (FT-IR) spectra before and after the ligand exchange confirmed

the presence of free –COOH from PAA (Figure S3). So it can be concluded that PAA is successfully bonded to the surface of UCNPs in place of oleic acid.

Under excitation at 980 nm, upconversion luminescence (UCL) spectrum of the PAA-capped $NaYF_4$:Yb^{3+},Er^{3+} exhibits three distinct emission bands at 524, 539 and 654 nm (Figure 1B), which originate from $^2H_{11/2} \rightarrow {}^4I_{15/2}$, $^4S_{3/2} \rightarrow {}^4I_{15/2}$ and $^4F_{9/2} \rightarrow {}^4I_{15/2}$ transitions of Er^{3+}, respectively.[35] The aqueous PAA-UCNPs shows a bright green emission by illuminated with a beam of near-infrared laser of 980 nm (the Inset Image in Figure 1B), because the green emission ranging from 510 to 560 nm is much stronger than the red emission at 654 nm as revealed by the upconversion spectrum.

3.2 Chemical reaction between NR and NO_2^-

The PAA-capped UNCPs do not have any physical and chemical interactions with nitrite, and do not also produce any spectral response to the presence of nitrite. In this work, neutral red (NR) is chosen as an aiding reactant for the detection of nitrite because it can selectively and efficiently react with nitrite[36] and causes the spectral change of PAA-capped UCNPs. Figure 2A illustrates the details of reaction between NO_2^- and NR. NO_2^- can selectively react with primary aromatic amine group in a strong acidic media to form a diazonium group. Interestingly, we found that when the aqueous media was adjusted to pH 6.0 with MES buffer, the diazonium group at the aromatic ring was extremely unstable and could be rapidly removed by releasing nitrogen at room temperature. Here, the final product is named as de-(NH_2) NR for the ease of description.

The reactive process can be clearly monitored by UV-vis absorption spectra and color changes of the reaction system. As shown in Figure 2B, pure NR in aqueous solution was red and exhibited a strong visible absorption at 525 nm. After the reaction with NO_2^- in presence of HCl, the solution quickly changed from red into blue, and displayed a visible absorption at 625 nm (Figure 2C). The red shift of absorption may be explained the formed diazonium group at the aromatic rings greatly extends the conjugation system. When the pH was buffered with MES to 6.0, it can be observed that the color of the solution gradually changed from blue to red, but the red was much lighter than the original red of NR. Simultaneously, the absorption at 625 nm shifted and returned to 545 nm (Figure 2D), and the light red color and absorption finally kept unchanged (data not shown). These observations clearly confirm the occurrence of reaction between NR and NO_2^-, and the process to form the initial diazonium group and final de-(NH_2) NR, as drawn in Figure 2A.

On the other hand, it was also observed that the absorption spectra were correlated with the final pH of diazonium salt solution. When the pH was 2.0, 3.0, 4.0, 5.0 and 6.0, the visible absorption gradually shifted from 625 to 545 nm, and the final color changed from blue to light red (Figure S4). This suggests that the decomposition amount of diazonium salt is dependent on the pH value of media. At the pH 6.0, the reaction could be rapidly completed and thus the solution color was finally stable in light red. Accordingly, the pH value is set at 6.0 for the following procedure of detection of NO_2^- in this study.

A
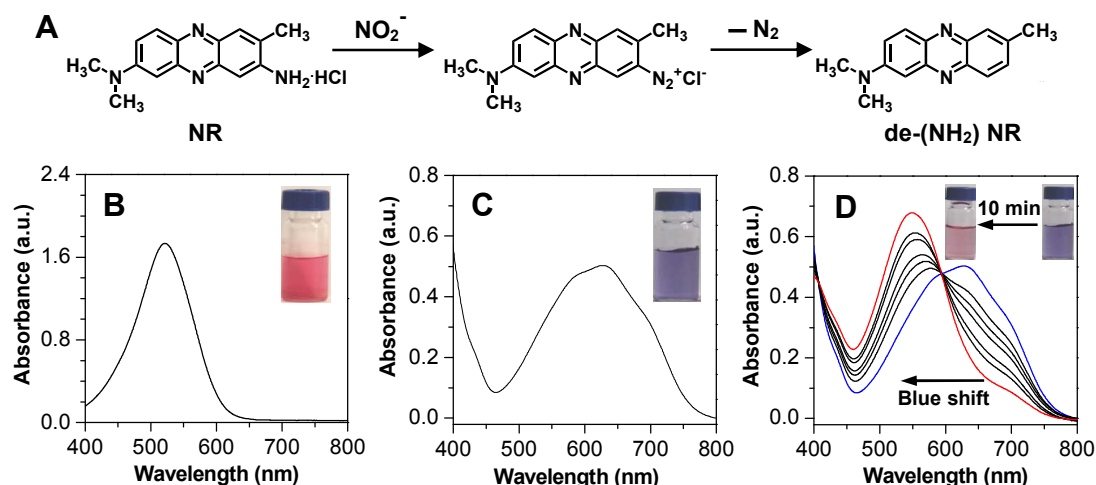
Fig. 2 (A) The reaction of neutral red (NR) with nitrite (NO_2^-) in water to form diazonium salt and lose the diazonium group. (B-D) The corresponding UV-vis spectra and color changes: (B) original NR solution; (C) diazonium salt solution; (D) the evolution of losing the diazonium group.
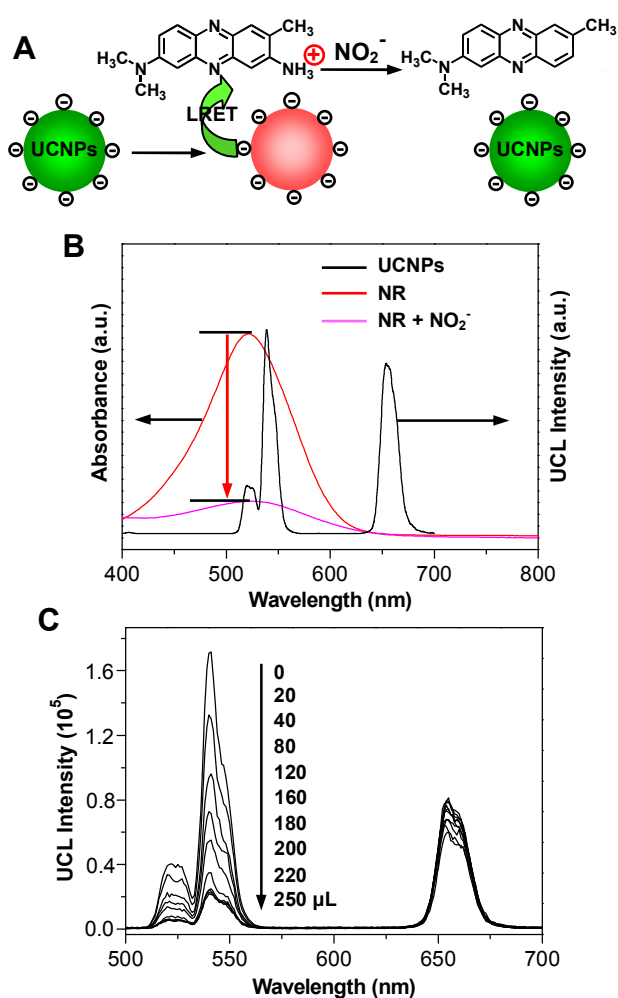
Fig. 3 (A) Schematic illustration for the principle of upconversion ratiometric fluorescence detection of NO_2^- with the aid of NR. (B) The spectral mechanism for the detection of NO_2^-: the upconversion spectrum of UCNPs (black line) and the UV-vis spectra of NR before (red line) and after (pink line) the reaction with NO_2^-. (C) The evolution of upconversion emission of PAA-capped UCNPs (0.08 mg/mL) upon the addition of NR (1.0 mM).

3.3 Upconversion luminescence mechanism for NO_2^- detection

Although the above spectral and colorful evolution can roughly indicate the presence of NO_2^-, it is difficult to be directly used for the quantitative and sensitive detection of NO_2^- because the small change in the absorption is easily interrupted by the background in real sample. On the basis of above reaction, we further proposed an upconversion ratiometric fluorescence detection of NO_2^- by an internal reference emission of UCNPs, in which the excitation of near-infrared laser avoided the background fluorescence and the internal reference emission greatly improved the accuracy of quantitative assay. Figure 3A illustrates the principle of upconversion ratiometric fluorescence detection of NO_2^- with the aid of NR. PAA-capped UCNPs are negatively charged due to the numerous -COOH groups on their surface, in which zeta potential value in MES buffer solution (pH 6.0) is tested to be -28.5 mV. NR molecules are positively charged due to the -NH_2 at aromatic ring, and thus NR molecules at acidic media can adsorb onto the surface of UCNPs by the opposite charge interaction. However, the absorption peak of NR exactly overlaps with the green emission of UCNPs (Figure 3B), and thus leads to the quench of green light by a luminescence resonance energy transfer (LRET). Meanwhile, the red emission of UCNPs remains unchanged and the color of UCNPs changes from green into red. When NR is transformed into de-(NH_2)-NR by the reaction with NO_2^-, the spectral absorption at 525 nm greatly decreases, and loses the interaction with PAA-capped UCNPs. As a result, the green emission is opened by shutting off the pathway of energy transfer. The recovery of green emission is dependent on the ratio of residual NR to de-(NH_2)-NR in the reaction system. Therefore, the ratiometric fluorescence from red to green can response to the amount of de-(NH_2)-NR in the system, providing a spectral detection of NO_2^-.

The upconversion luminescence (UCL) quenching behavior was firstly studied and the results are shown in Figure 3C. The green emission of PAA-capped UCNPs at 539 nm decreased gradually upon the addition of NR and was nearly completely quenched. Meanwhile, the red emission at 654 nm only slightly

decreased due to the dilution of solution volume after the addition of NR. That is to say, the red emission of PAA-UCNPs kept the original intensity. The ratio of luminescence intensity (I_{539}/I_{654}) exhibits a good linear correlation with the amount of NR (Figure S5). These observations confirm the quenching mechanism of UCNPs with NR, as shown in Figure 3A.
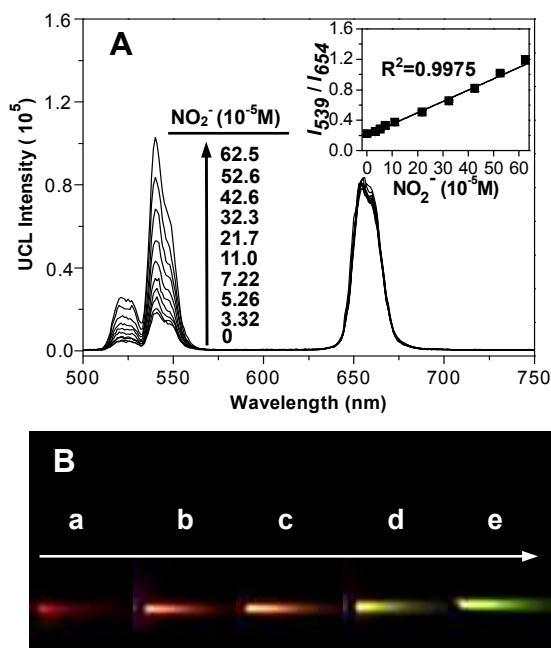

Fig. 4 (A) The evolution of upconversion spectra of NR-UCNPs system (λ_{ex} = 980 nm) with the increase of NO_2^- concentrations. The inset is the calibration curve of I_{539}/I_{654} versus the NO_2^- concentrations. (B) The visual color evolution from red to orange yellow and final green after the addition of NO_2^- with the concentrations of (a) 0, (b) 5.26, (c) 11.0, (d) 42.6 and (e) 62.5×10^{-5} M (The images are taken under the illumination of 980-nm laser).

3.4 Upconversion ratiometric fluorescence detection of NO_2^-

The detection of NO_2^- was performed by a two-step procedure. In the first step, different amounts of NO_2^- aqueous solution were mixed with 210 μL of 1.0 mM NR and 60 μL of 1.0 M HCl. The reaction was completed in 10 min at room temperature by vigorously stirring. In the second step, the above mixture was buffered to pH 6.0 by MES solution, and then 25 μL of 10 mg/mL PAA-capped UCNPs aqueous solution was added followed by adjusting the volume of the system to 3.0 mL. The details about the amount of experimental reagents were described in the supporting information, and the results are shown in Figure S6-S8.

Then the sensing ability of NR-UCNPs system for NO_2^- detection is investigated by UCL spectroscopy. As illustrated in Figure 4A, in the presence of different NO_2^- concentrations (0, 3.32, 5.26, 7.22, 11.0, 21.7, 32.3, 42.6, 52.6, and 62.5×10^{-5} M), the green emission of UCNPs at 539 nm continuously recovered under excitation at 980 nm, and about 4.7-fold luminescence enhancement was measured when the concentration of NO_2^- reached to 62.5×10^{-5} M. The luminescence intensity enhancement of UCNPs with the increasing amounts of NO_2^- is attributed to the decrease of the LRET efficiency. It can be seen from Figure S9 that with the increasing amounts of NO_2^-, the spectral overlap between the green emission of UCNPs at 539 nm and absorption

of NR at 525 nm gradually reduces, causing a decrease in the LRET from the PAA-capped UCNPs to NR. Consequently, the green emission of UCNPs increases with the increase of NO_2^- concentration. Using upconversion emission at 539 nm as detection signal (Figure S10), the detection limit for NO_2^- is measured to be 16.1 μM (0.7 ppm) based on the definition of three times the deviation of the blank signal (3σ).

It should be noted that during the reaction process with NO_2^-, no significant changes in the luminescence intensity at 654 nm are measured, thus the red emission band can be used as the reference standard. Herein, the ratio of the two intensities (I_{539}/I_{654}) is also chosen as detection signal, where has a good linear correlation between I_{539}/I_{654} and the concentration of NO_2^- (inset in Figure 4A). The line arregression equation is described by the following equation: $I_{539}/I_{654} = 0.20209 + 0.01584$ C (where C is the concentration of NO_2^- in $\times 10^{-5}$ M) and the correlation coefficient is 0.9975. And the limit of detection (3σ) for NO_2^- can reach as low as 4.67 μM (0.2 ppm), which is much lower than the maximum permitted contamination levels of nitrite in drinking water and meat products (1 ppm and 200 ppm, respectively). Some recent published literatures also reported the lower detection limit of nitrite using different detection methods.[19-22] Such as fluorescent gold nanoclusters can dectect 1 nM of nitrite[19] and reaction based fluorometric probes can detect as low as 1.5 ppb of nitrite,[21] respectively. Here, using our unoptimized upconversion nanoparticles probe can detect 4.67 μM (0.2 ppm) of nitrite based on an efficient reaction between NO_2^- and NR, which revealed that this analysis method will show a specific response to NO_2^- while avoids interference from other materials.

Moreover, a small variation in the ratio of the two intensities (I_{539}/I_{654}) leads to a clear color evolution from red to orange yellow and final bright green, which can be easily observed with the naked eye under excitation at 980 nm (Figure 4B). These facts indicate that ratiometric upconversion luminescence detection is more favorable. Furthermore, HSV (Hue, Saturation, Value) is a commonly used cylindrical color-space in digital imaging. The hue parameter is shown to be accessible for convenient quantitative fluorescence imaging and has been applied to the quantification of a pH-sensitive dye by Hakonen and co-workers.[37] Therefore, we also studied the hue based quantification of nitrite ions (Figure S11). The result shows a good linear correlation between the hue and the concentration of NO_2^-.

To evaluate the level of selectivity of the present ratiometric sensor for NO_2^- over other ions, such as some cations (Zn^{2+}, Mg^{2+}, Ca^{2+}, Mn^{2+}, Ba^{2+}, Cu^{2+}, Cd^{2+}, Ni^{2+}, NH_4^+) and anions (NO_3^-, F^-, Cl^-, Br^-, Ac^-, SO_4^{2-}), the green emission intensity of UCNPs was measured by UCL spectroscopy. It can be found that with the addition of NO_2^- at 62.5×10^{-5} M, the green emission of UCNPs at 539 nm was turned on, while the red emission at 654 nm kept unchanged, leading to the increase of the intensity ratio (I_{539}/I_{654}) (Figure 5). As for other ions, even when the concentration of those ions ranged up to 62.5 mM, the green emission at 539 nm stayed nearly unchanged, accompanied by no variation in the intensity ratio (I_{539}/I_{654}), indicating these ions have no interaction with NR. Moreover, the anti-interference test of this NO_2^- sensor is also carried out in the presence of other ions. The intensity ratio (I_{539}/I_{654}) with the addition of NO_2^- (62.5×10^{-5} M) was

unaffected by 100-fold excesses of the interfering ions (Figure 5), indicating that the sensing of the proposed method for NO_2^- is not affected by these common coexistent ions.
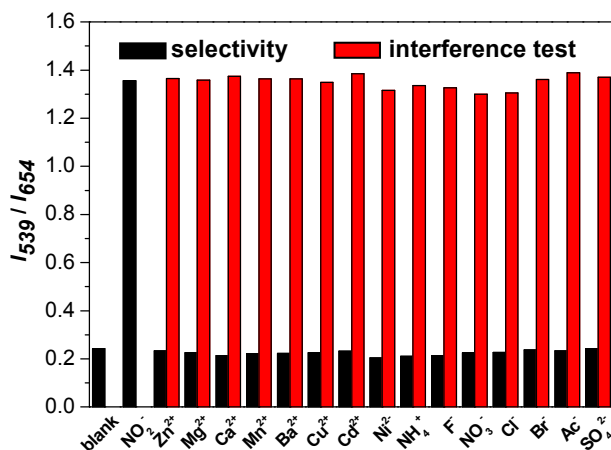
[5] **Fig. 5** Selectivity (black bar) and interference test (red bar). The selectivity data were obtained using 62.5 mM cations/anions and 62.5×10^{-5} M NO_2^-. The anti-interference tests were performed by the addition of 62.5×10^{-5} M NO_2^- in the coexistence of an excess of interfering ions (62.5 mM).

[10] Similarly, the excellent selectivity and anti-interference of our ratiometric probe for NO_2^- were simultaneously tested by UV-vis absorption spectroscopy (Figure S12). NO_2^- with the concentration of 62.5×10^{-5} M can react with NR, and then sharply decreases the absorption intensity of NR at 525 nm. As for other [15] ions, nearly no variations of absorption intensity at 525 nm are observed. In addition, the interference experiment of this NO_2^- sensor was carried out in the presence of the above ions. The results showed that the decrease of the absorption intensity at 525 nm resulting from the reaction between NO_2^- and NR was not [20] influenced by the existence of other ions tested.

All of the above indicate that our upconversion turn-on probe possesses excellent selectivity and anti-interference for NO_2^- determination, and therefore can be used as a ratiometric fluorescence sensor for ultra-selective detection of NO_2^- in [25] environmental samples without interferences from other ions.

Table 1. Determination of NO_2^- in tap water, lake water and cured meat samples[a]

spiked concentration $(10^{-5}$ M)	Tap water		Lake water		Cured meat	
	Found $(10^{-5}$M)	Recovery (%)	Found $(10^{-5}$M)	Recovery (%)	Found $(10^{-5}$M)	Recovery (%)
21.7	20.78	95.76±2.1	19.74	90.97±2.9	23.27	107.24±3.2
42.6	43.17	101.34±1.9	41.19	96.69±1.7	43.03	101.01±2.5
52.6	52.45	99.71±1.5	53.14	101.03±1.5	54.48	103.57±1.9

[a] Values shown were the calculated mean NO_2^- concentration for each [30] sample and were determined from three replicates.

3.5 Practical application in real samples

To assess the utility of the proposed NO_2^--responsive ratiometric sensor, it was applied to detect NO_2^- in real samples, including tap water, lake water and cured meat. Tap water and lake water were [35] filtered through 0.45 μm Supor filters to remove any particulate suspension. As for the meat sample, 20 g of cured meat was crushed and mixed well with 20 mL of ultrapure water. The mixture was stayed under ambient condition for one day, centrifuged at 3000 r/min and then filtrated through 0.45 μm [40] Supor filters to remove the insoluble draff. Before the spiking of NO_2^-, we firstly detected the sample solution used the Griess method and no NO_2^- was detected. For real sample detection, 6.9 mg of sodium nitrite was respectively added into 10 mL of the three well-prepared sample filtrate. Then different volume (6, 12 [45] and 15 μL) of the sample solution was mixed with 210 μL of neutral red (1.0 mM) and 60 μL of HCl (1.0 M) under rotation for 10 min. After the reaction, the mixture was buffered to pH 6.0, followed by addition of PAA-capped UCNPs aqueous solution (25 μL, 10 mg/mL). Finally, the volume of the system was [50] diluted to 3.0 mL, and the UCL spectra were measured in triplicate to accurately estimate the NO_2^- quantitatively. The concentrations of spiked NO_2^- were calculated to be 21.7, 42.6 and 52.6×10^{-5} M, respectively. However, the found amounts of NO_2^- were obtained from the linear plot between the ratio [55] (I_{539}/I_{654}) and the concentration of NO_2^-, and the averages with standard deviation were presented in Table 1. It can be seen that the found concentrations of NO_2^- in the real samples determined by the proposed method were in good agreement with the spiked concentrations of NO_2^-, along with the quantitative recoveries [60] being to 90.97-107.24%, which indicated the reliability and practicality of this upconversion switching method for ratiometric fluorescence detection of NO_2^- in complicated real samples.

4. Conclusions

In summary, using upconversion nanoparticles and an efficient [65] reaction, a selective upconversion switching method for the ratiometric fluorescence detection of NO_2^- was developed. This upconversion nanosensor is successfully applied in the real samples analysis with relatively satisfactory recovery. Because of the near-infrared excitation, the upconversion probe can [70] efficiently avoid autofluorescence interference, and thus may provide the more potential applications for the detection of nitrite salts in biological samples.

Acknowledgments

Notes and References

[80] [a] Department of Chemistry, University of Science & Technology of China, Hefei, Anhui 230026, China
[b] Institute of Intelligent Machines, Chinese Academy of Sciences, Hefei, Anhui 230031, China
[c] Fujian Inspection and Research Institute for Product Quality, Fuzhou, [85] Fujian 350002, China
† Electronic Supplementary Information (ESI) available. See DOI: 10.1039/b000000x/

1 Z. P. Chen, Z. Y. Zhang, C. L. Qu, D. W. Pan and L. X. Chen, *Analyst,* [90] 2012, **137**, 5197-5200.
2 M. T. Gladwin, J. H. Crawford and R. P. Patel, Free Radical Biol. Med., 2004, 36, 707–717.

3 B. A. Kilfoy, Y. W. Zhang, Y. Park, T. R. Holford, A. Schatzkin, A. Hollenbeck and M. H. Ward, *Int. J. Cancer,* 2011, **129**,160-172.

4 R. K. Hanajiri, R. S. Martin and S. M. Lunte, *Anal. Chem.,* 2002, **74**, 6370-6377.

5 D. M. Manassaram, L. C. Backer and D. M. Moll, *Environ. Health Perspect.,* 2006, **114**, 320-324.

6 United States Environmental Protection Agency, National Primary Drinking Water Regulations: Contaminant Specific Fact Sheets, Inorganic Chemicals, Consumer Version, Washington, DC, 2009.

7 M. J. Focazio, D. Tipton, S. D. Shapiro and L. H. Geiger, *Ground Water Monit. Rem.,* 2006, **26**, 92-104.

8 European Standard. Water quality-determination of nitrites molecular absorption spectrometric method, EN 26777; European Standard: Pilsen Czech Republic, 1993.

9 Z. Lin, W. Xue, H. Chen and J. M. Lin, *Anal. Chem.,* 2011, **83**, 8245-8251.

10 D. Tsikas, A. Schwarz and D. O. Stichtenoth, *Anal. Chem.,* 2010, **82**, 2585-2587.

11 C. Merusi, C. Corradini, A. Cavazza, C. Borromei and P. Salvadeo, *Food Chem.,* 2010, **120**, 615-620.

12 M. Pietrzak and M. E. Meyerhoff, *Anal. Chem.,* 2009, **81**, 3637-3644.

13 E. Pagliano, J. Meija, R. E. Sturgeon, Z. Mester, and A. D'Ulivo. *Anal. Chem.,* 2012, **84**, 2592-2596.

14 J. Zhang, C. Yang, X. L. Wang and X. R. Yang. *Analyst,* 2012, **137**, 3286-3296.

15 H. J. Zhang, S. D. Qi, Y. L. Dong, X. J. Chen, Y. Y. Xu, Y. H. Ma and X. G. Chen, *Food Chem.,* 2014, **151**, 429-434.

16 N. Adarsh, M. Shanmugasundaram, and D. Ramaiah. *Anal. Chem.,* 2013, **85**, 10008-10012.

17 W. L. Daniel, M. S. Han, J. S. Lee, and C. A. Mirkin, *J. Am. Chem. Soc.,* 2009, **131**, 6362–6363.

18 N. Xiao and C. X. Yu, *Anal. Chem.,* 2010, **82**, 3659-3663.

19 H. Y. Liu, G. H. Yang, E. S. Abdel-Halim and J. J. Zhu. *Talanta*, 2013, **104**, 135-139.

20 Q. L. Yue, L. J. Sun, T. F. Shen, X. H. Gu, S. Q. Zhang and J. F. Liu. *J Fluoresc.,* 2013, **23**, 1313-1318.

21 C. Liu, X. Y. Qiu, J. Zhao and Y. L. Yang. *Anal. Methods*, 2014, 6, 463-468.

22 V. Kumar, M. Banerjee and A. Chatterjee. *Talanta,* 2012, **99**, 610-615.

23 F. Auzel, *Chem. Rev.,* 2004, **104**, 139-174.

24 H. S. Mader, P. Kele, S. M. Saleh and O. S. Wolfbeis, *Curr. Opin. Chem. Biol.,* 2010, **14**, 582-596.

25 W. Feng, L. D. Sun, Y. W. Zhang and C. H. Yan, *Coord. Chem. Rev.,* 2010, **254**, 1038-1053.

26 Y. S. Liu, D. T. Tu, H. M. Zhu and X. Y. Chen. *Chem. Soc. Rev.,* 2013, **42**, 6924-6958.

27 F. Wang, D. Banerjee, Y. S. Liu, X. Y. Chen and X. G. Liu. *Analyst,* 2010, **135**, 1839-1854.

28 M. Wang, C. C. Mi, W. X. Wang, C. H. Liu, Y. F. Wu, Z. R. Xu, C. B. Mao and S. K. Xu, *ACS Nano,* 2009, **3**, 1580-1586.

29 S. A. Hilderbrand, F. W. Shao, C. Salthouse, U. Mahmood and R. Weissleder, *Chem. Commun.,* 2009, 28, 4188-4190.

30 Y. Liu, M. Chen, T. Y. Cao, Y. Sun, C. Y. Li, Q. Liu, T. S. Yang, L.M. Yao, W. Feng and F. Y. Li, *J. Am. Chem. Soc.,* 2013, **135**, 9869-9876.

31 C. X. Li, J. L. Liu, S. Alonso, F. Y. Li and Y. Zhang, *Nanoscale,* 2012, **4**, 6065-6071.

32 R. R. Deng, X. J. Xie, M. Vendrell, Y. T. Chang and X. G. Liu, *J. Am. Chem. Soc.,* 2011, **133**, 20168-20171.

33 Z.Q. Li and Y. Zhang, *Nanotechnology,* 2008, **19**, 345606-345610.

34 C. Wang, L. Cheng, Y. M. Liu, X. J. Wang, X. X. Ma, Z. Y. Deng, Y. G. Li and Z. Liu, *Adv. Funct. Mater.,* 2013, **23**, 3077-3086.

35 G. F. Wang, Q. Peng and Y. D. Li, *Acc. Chem. Res.,* 2011, **44**, 322-332.

36 G. Z. Liu, M. Chockalingham, S. M. Khor, A. L. Gui and J. J. Gooding, *Electroanalysis,* 2010, **22**, 918-926.

37 A. Hakonen, J. E. Beves and N. Strömberg, *Analyst,* 2014, DOI: 10.1039/c4an00063c.
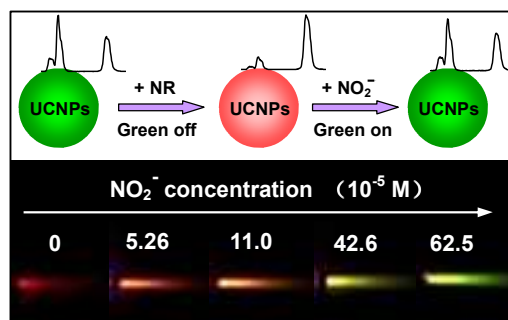
Individual upconversion nanoparticles with green and red emissions were synthesized and used the ratiometric fluorescence probes for the detection of nitrite by selectively turning on the green fluorescence.